

# Synthesis and characterisation of chemical bath deposited TiO<sub>2</sub> thin-films

P. Manurung<sup>a</sup>, Y. Putri<sup>a</sup>, W. Simanjuntak<sup>b</sup>, I.M. Low<sup>c,\*</sup>

<sup>a</sup>Department of Physics, FMIPA, The University of Lampung, Bandar Lampung 35145, Indonesia

<sup>b</sup>Department of Chemistry, FMIPA, The University of Lampung, Bandar Lampung 35145, Indonesia

<sup>c</sup>Department of Applied Physics, Curtin University, GPO Box U1987, Perth, WA 6845, Australia

Received 21 May 2012; accepted 7 June 2012

Available online 18 June 2012

## Abstract

A series of titania thin films was prepared by chemical bath deposition (CBD) of TiCl<sub>3</sub> on indium tin oxide (ITO) glass at room temperature, followed by calcinations at 500 °C for 4 h. The effect of cyclic deposition on phase composition, microstructure and electrical resistivity of TiO<sub>2</sub> thin films was characterised using X-ray diffraction, scanning electron microscopy and four-point probe respectively. Results showed that TiO<sub>2</sub> films produced by single deposition cycle were amorphous. In contrast, those produced by 5 and 6 deposition cycles were partly amorphous and partly crystalline with the formation of rutile. Both the film thickness and electrical resistivity increased with an increase in the number of deposition cycles.

Crown Copyright © 2012 Published by Elsevier Ltd and Techna Group S.r.l. All rights reserved.

**Keywords:** B. Microstructure; Chemical bath deposition; Rutile; Amorphous

## 1. Introduction

Thin-films are important components of various devices widely used in electronic, protective, membrane and sensor applications. The most common preparation method of thin-films is chemical deposition since it offers several advantages such as low cost, and the ability to produce samples with large surface area [1]. Some authors [1,2] have reported various aspects of chemically deposited thin films, while others [3,4] have studied the effects of varying the growth parameters such as deposition rates, bath compositions and bath temperature on the microstructures and properties of thin films.

TiO<sub>2</sub> exists in three main phases: anatase, brookite and rutile where the latter is a stable phase. This oxide is an attractive material due to its wide applications, such as in paints, sunscreens, and as photocatalyst under ultra-violet light [5–7]. Hitherto, the synthesis of TiO<sub>2</sub> thin films or bulk has led to the emergence of nanoscience and

nanotechnology by virtue of their superior physical and chemical properties [8,9].

In this paper, we have used chemical bath deposition to synthesize a series of titania thin films on indium tin oxide (ITO) glass and investigated the effect of cyclic deposition on phase composition, microstructure and electrical resistivity of TiO<sub>2</sub> thin films.

## 2. Experimental details

TiO<sub>2</sub> thin-films were synthesized using the solution of titanium trichloride (TiCl<sub>3</sub>) and NaHCO<sub>3</sub>. The process of deposition was carried out by dropwise addition of freshly prepared NaHCO<sub>3</sub> solution into TiCl<sub>3</sub> solution in a beaker glass, and then stirred until a pH of 3–4 was reached. The ITO glass substrate (35 × 15 × 1 mm<sup>3</sup>) was hung vertically until 2 cm of the substrate was immersed into the solution of TiCl<sub>3</sub> and NaHCO<sub>3</sub>. The solution was stirred for up to 6 h, depending on the number of deposition cycles to produce 6 samples, as shown in Table 1. The samples were then dried at 100 °C for 1 h, followed by calcination at 500 °C for 4 h.

\*Corresponding author. Tel.: +61 8 9266 7544; fax: +61 8 9266 2377.

E-mail addresses: [j.low@curtin.edu.au](mailto:j.low@curtin.edu.au),  
[low246@gmail.com](mailto:low246@gmail.com) (I.M. Low).

Table 1  
Formulations of samples as a function of deposition cycle during processing.

Sample	Number of deposition cycles	Deposition time per cycle (h)
A	1	6
B	2	3
C	3	2
D	4	1.5
E	5	1.2
F	6	1

Table 2  
Relative peak intensities of anatase (101) and rutile (110) for various TiO<sub>2</sub> thin films deposited on ITO.

Sample	Anatase (101)	Rutile (110)	ITO
A	Not detected	Not detected	Strong
B	Not detected	Not detected	Strong
C	Not detected	Not detected	Strong
D	Not detected	Weak	Moderate
E	Not detected	Weak	Moderate
F	Not detected	Strong	Moderate

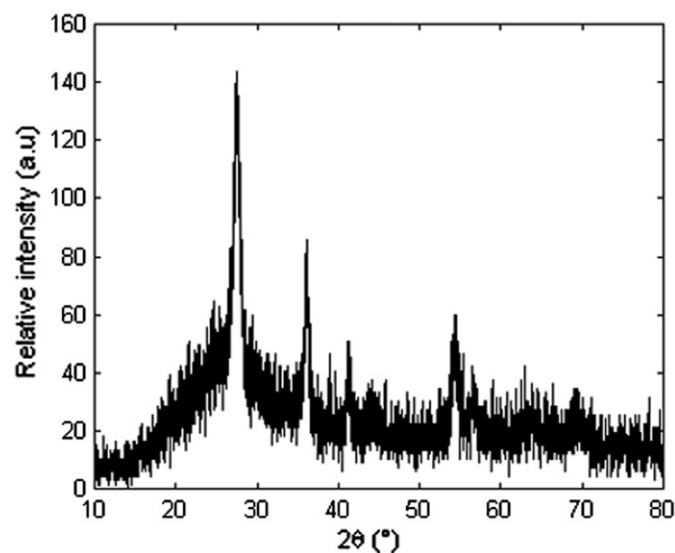


Fig. 1. XRD plot for sample F with six cycles of deposition. [Legend: r=rutile].

X-ray diffraction data were collected using a Shimadzu 610 diffractometer. The operating conditions used were CuK $\alpha$  radiation ( $\lambda=1.54506$  Å) produced at 40 kV and 30 mA. The diffraction patterns were collected over the  $2\theta$  range 10–80°. A JEOL JSM-6360LA scanning electron microscope was used to examine the microstructures of surface and cross-sections of the samples. The electrical resistivity ( $\rho$ ) of TiO<sub>2</sub> thin-films were measured using the four-point probe method.

### 3. Results and discussion

#### 3.1. Phase composition

It was found that the color of TiO<sub>2</sub> thin-films is clear or transparent and adheres well to the ITO glass substrate. Visually the films are homogenous with smooth surface appearance. The XRD spectra were collected for samples A, D and F. The XRD data was also collected on ITO glass as a control. The diffraction pattern of sample F is shown in Fig. 1 which depicts the existence of rutile only in the thin-film of TiO<sub>2</sub>. In all samples, only rutile was

detected and no peaks due to anatase (101) were detected probably due to their transformation to rutile during sintering at 500 °C for 4 h. Table 2 shows the phase analysis of anatase and rutile in all the samples prepared according to conditions stated in Table 1.

It should be mentioned that the normal XRD is not ideal for characterising the phase compositions of thin-films due to relatively high penetrating ( $\geq 30$  μm) depth of X-rays in symmetric mode. Since the TiO<sub>2</sub> thin-films produced in this study are less than 5 μm thick, the X-rays will penetrate into the ITO substrate and produce an undesirable strong background noise due to the amorphous nature of ITO. Hence, it will be more accurate to use grazing-incidence XRD to probe their near-surface phase compositions of TiO<sub>2</sub> thin-films. The critical angle ( $\alpha_c$ ) for grazing-incidence diffraction can be approximated by [10]:

$$\alpha_c = 1.6 \times 10^{-3} \rho \lambda$$

where  $\alpha_c$  is in radians,  $\rho$  is density of TiO<sub>2</sub> (rutile=4.25 g/cm<sup>3</sup>) and  $\lambda$  is wavelength in Å. Hence the calculated value of  $\alpha_c$  for TiO<sub>2</sub> thin films is 0.010472 or 0.6°. Above the critical angle, the penetration depth ( $d$ ) can be calculated from [11]:

$$d = 2 \alpha / \mu$$

where  $\mu$  is the linear absorption coefficient of matter. Since the value of  $\mu$  for rutile is 907.0775/cm [12] and the normal XRD uses an incidence angle of 8°, penetration depth of X-rays will be  $\sim 30.8$  μm which is deeper than the thickness of the thin-films. As a result, the X-rays will also detect the ITO glass and give rise to undesirable large amorphous background.

By using the Scherrer equation [13], one can determine the crystallite size of this sample. By taking the width of diffraction peak into consideration, the crystallite size of TiO<sub>2</sub> in sample F was determined to be  $\sim 10$  nm. This value is much less than the particle size of  $\sim 200$  nm indicated by the SEM image (Fig. 2d). Since particles or grains are made up of small crystallites, this suggests that there are about 20 crystallites in each TiO<sub>2</sub> particle on sample F.

The PDF file number 21–1276 for rutile from the database was used to identify the phases formed [14]. According to Lokhande [15], there is no difference between ITO glass and TiO<sub>2</sub> having low grade of crystallinity. In

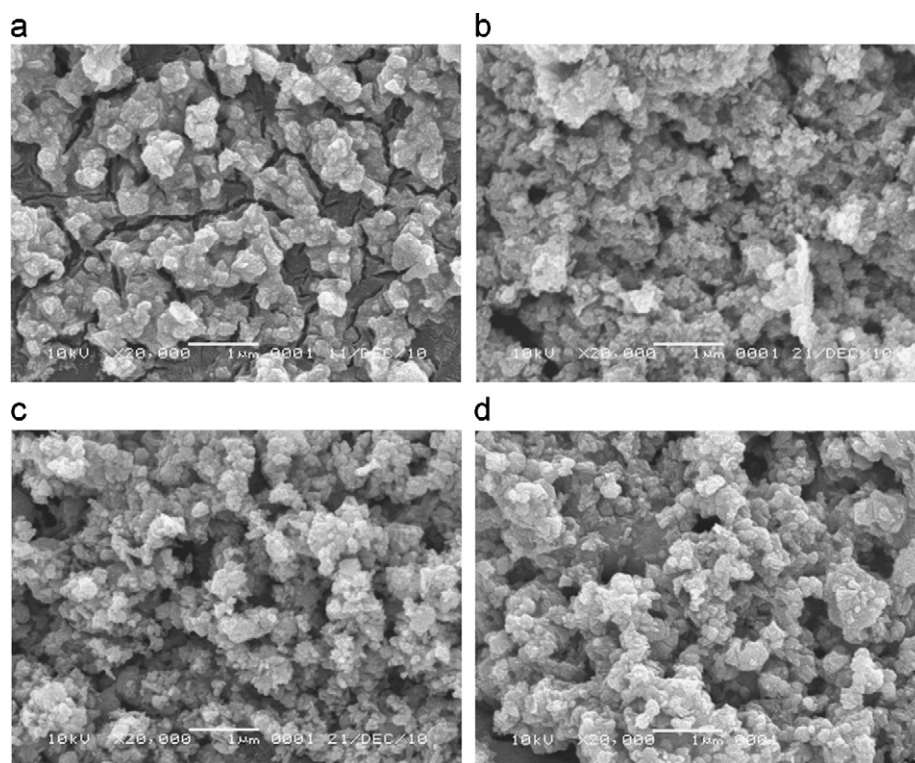


Fig. 2. SEM images of samples with various processing conditions: (a) sample A (1 cycle at 6 h), (b) sample B (2 cycles at 3 h), (c) sample D (4 cycles at 1.5 h), and (d) sample F (6 cycles at 1 h).

fact, it is not necessary for  $\text{TiO}_2$  to have a high grade of crystallinity when it is used in applications such as a photodetector [16].

### 3.2. Microstructure

The SEM images of  $\text{TiO}_2$  thin films prepared by multiple depositions are shown in Fig. 2. These images clearly show distinct contrast in microstructures in films prepared between one and six deposition cycles. This indicates that the number of deposition cycles can lead to a significant change in the microstructures of  $\text{TiO}_2$  films.

The microstructures of the thin-films shown in Fig. 2 are for samples with 1, 2, 4 and 6 deposition cycles. It is interesting to note that the microstructures for thin-films prepared from 1 to 4 cycles are quite similar although cracking can be seen in sample A with one deposition cycle. In films prepared from 4 and 6 deposition cycles, the cracks had disappeared and the amount of pores also decreased. It appears that multiple depositions had helped to fill the pores within the  $\text{TiO}_2$  layer thus making the surface denser. If the film remains attached to the substrate and does not crack during sintering, shrinkage in the plane of the substrate can be inhibited. The stresses that arise during the sintering of constrained films are analogous to those in a sandwich seal caused by mismatch in the thermal expansion coefficients in the layers.

It is interesting to note that the films have pores distributed all over the surfaces. These pores can play the

role of enhancing dye-sensitization when the  $\text{TiO}_2$  films are used for solar cell application [17] as the dye can fill the pores. Dye can also absorb the incident ray and inject electrons to the  $\text{TiO}_2$  semiconductor.

Furthermore, samples were also observed using SEM in cross-sectional view from top surface of the film to the ITO glass in order to estimate the film thickness. Microstructures of samples A, B and E are shown in Fig. 3. Using the scale-bar on each image, one can estimate the film thickness deposited on the substrate. The variation of film thickness as a function of deposition cycles is depicted in Fig. 4. By taking into account the two estimated standard deviations, the thickness of the films can be observed to increase with the number of deposition cycles. This is self-evident because when repeated depositions were done, the material deposited on the substrate also increased. From this figure one can tailor-design the thickness of the film based on number deposition cycles.

### 3.3. Electrical resistivity

The electrical resistivity or conductivity of  $\text{TiO}_2$  films was measured using four-point probes. By knowing the resistivity one can infer whether film produced is a conductor or semiconductor. The application of  $\text{TiO}_2$  as photo-conductor must have properties of a semiconductor because a conductor has no band-gap energy. If the incident ray overcomes the band-gap energy, electrical

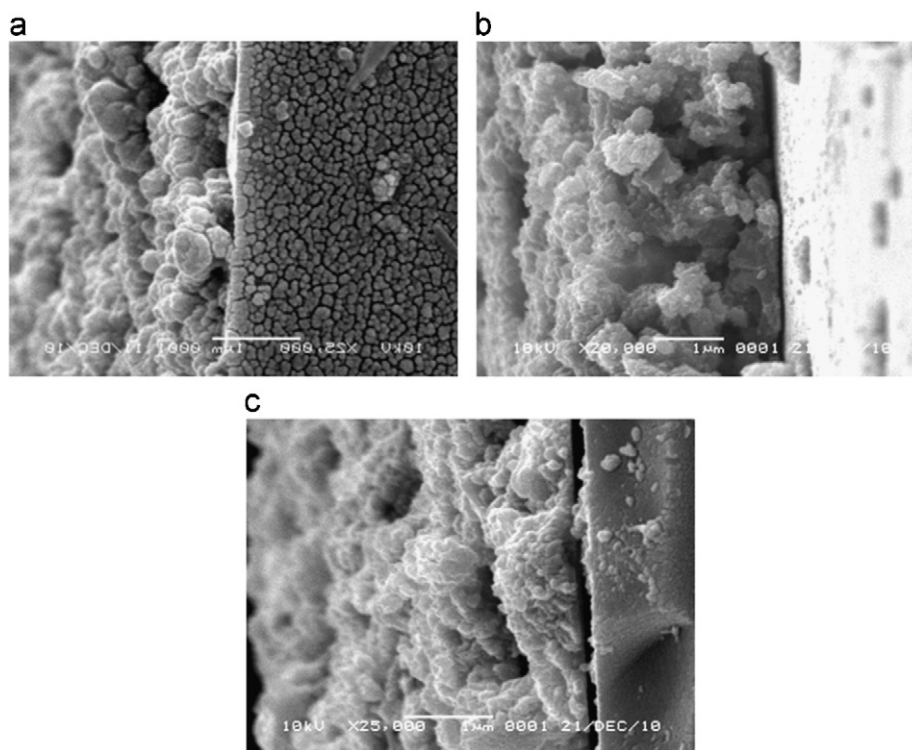


Fig. 3. SEM images showing the cross-sectional view from of samples from top-surface to the ITO glass substrate where the  $\text{TiO}_2$  layer is on the left and the ITO glass is on the right. (a) sample A, (b) sample B and (c) sample E.

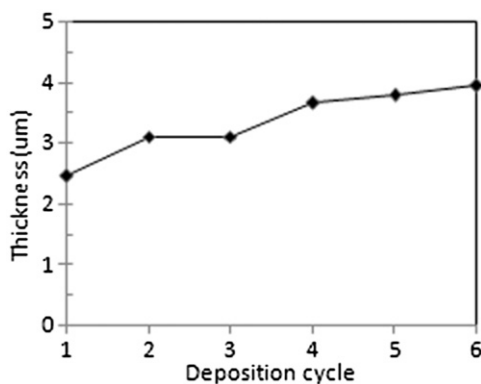


Fig. 4. Variations of film thickness as a function of deposition cycle.

conduction will occur. The variation of electrical resistivity as a function of deposition cycles is depicted in Fig. 5.

The resistivities of conductors and semiconductors normally range from  $10^{-3}$  to  $10^8 \Omega\text{-cm}$  [18]. Based on this value, the resistivity of  $\text{TiO}_2$  thin-films synthesized in this study can be classified as a semiconductor. Since the resistivity increases with deposition cycles, this indicates that multiple depositions serve to increase the resistivity by virtue of more pores and materials being deposited in the film as the thickness increases. When the deposited material increases, the resistivity of a layer increases with each deposition cycle. It has been reported that the resistivity value of  $\text{TiO}_2$  thin films prepared by DC magnetron sputtering ranged from  $10^7$  to  $10^{10} \Omega\text{-cm}$  [19].

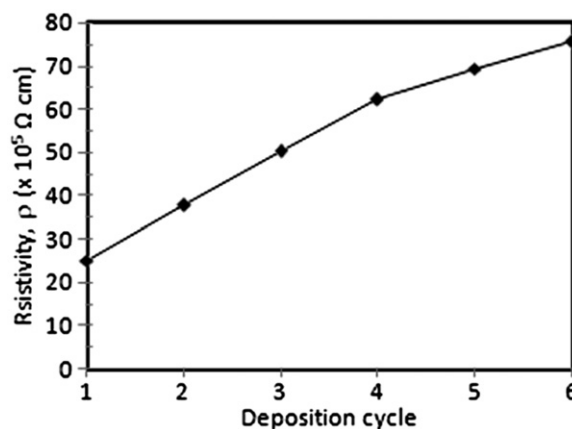


Fig. 5. Variations of electrical resistivity of  $\text{TiO}_2$  films as a function of deposition cycle.

Thus, the resistivity results obtained in this work are comparable to results reported in the literature.

#### 4. Conclusions

Thin-films of  $\text{TiO}_2$  produced by multiple depositions were more crystalline with rutile being the only phase formed. In contrast,  $\text{TiO}_2$  films produced by single deposition cycle were amorphous. Both the film thickness and electrical resistivity of  $\text{TiO}_2$  increased with an increase in the number of deposition cycles.

## Acknowledgements

The authors thank the University of Lampung for financial support and access to various analytical facilities.

## References

- [1] J.Y. Choi, K.J. Kim, J.B. Yoo, D. Kim, Properties of cadmium sulphide films deposited by chemical bath deposition with ultrasonication, *Solar Energy* 64 (1998) 41–45.
- [2] B.R. Ortega, D. Lincot, Chemical deposition of cadmium sulphide thin films in the ammonia thiourea system, *Journal of the Electrochemical Society* 140 (1993) 3464–3468.
- [3] F.C. Eze, C.E. Okeke, Chemical bath deposited cobalt sulphide films; preparation effects, *Materials Chemistry and Physics* 47 (1997) 31–33.
- [4] P.J. Sabastian, H. Hu, Identification of the impurity phase in chemically deposited CdS thin films, *Advanced Materials for Optics and Electronics* 4 (1994) 407–409.
- [5] A. Fujishima, K. Honda, Electrochemical photolysis of water at a semiconductor electrode, *Journal Nature* 238 (1972) 37–38.
- [6] A. Fujishima, T.N. Rao, D.A. Tryk, Titanium dioxide photocatalysis, *Journal of Photochemistry and Photobiology C: Photochemistry Reviews* 1 (2000) 1–21.
- [7] D.A. Tryk, A. Fujishima, K. Honda, Recent topics in photoelectrochemistry: achievements and future prospects, *Electrochimica acta* 45 (15–16) (2000) 2363–2267.
- [8] M. Tejos, G.E. Buono-Cuore, F.R. Diaz, M.A. Del Valle, J.J. Palomares, Direct photodeposition of nanostructured TiO<sub>2</sub> thin film from B-Diketonate complexes and their photocatalytic behaviour, *Journal of the Chilean Chemical Society* 49 (2004) 297–301.
- [9] D. Reyes-Coronade, G. Rodriguez-Gattorno, M.E. Espinosa-Pesqueira, C. Cab, R. De Ros, G. Oskam, Phase-pure TiO<sub>2</sub> Nanoparticles: anatase, brookite and rutile, *Nanotechnology* 19 (2008) 1–6.
- [10] P. Barner, Dynamic diffraction studies on the synthesis of ceramics using synchrotron radiation, *Transactions and Journal of the British Ceramic Society* 91 (1992) 26–29.
- [11] G.H. Vineyard, Grazing-incidence diffraction and the distorted-wave approximation for the study of surfaces, *Physical Review B* 26 (1982) 4146–4158.
- [12] H.A. Liebhafsky, H.G. Pfeiffer, E.H. Winslow, P.D. Zeman, X-Ray, Electrons and Analytical Chemistry, Wiley-Interscience, New York, 1972 525–528.
- [13] B.D. Cullity, Elements of X-Ray Diffraction, Addison-Wesley Publishing Company, 1978 105.
- [14] National Bureau of Standards (US), Monography 25.7, 83 (1969), PCPDFWIN Version 1.30. 1997.
- [15] C.D. Lokhande, K. Eun-Ho, Shimjao Deong, Room temperature chemical deposition of amorphous TiO<sub>2</sub> thin film from Ti (III) chloride solution, *Journal of Materials Science* 39 (2004) 2915–2918.
- [16] Y.C. Lee, Z. Hasan, F.K. Yam, K. Ibrahim, M.E. Kordes, W. Halven, P.C. Colter, Characteristics of low temperature growth GaN on Si (III), *Journal of Solid State Communications* 133 (2005) 283–287.
- [17] G. Phani, G. Tulloch, I. Vittorio, I. Skyrabbin, Titania solar cells: new photovoltaic technology, *Renewable Energy* 22 (1) (2001) 303–309.
- [18] S.M. Sze, Semiconductor Devices: Physics and Technology, John Wiley & Sons, 1985 1.
- [19] M. Stamate, I. Vascan, I. Lazar, G. Lazar, I. Caraman, M. Caraman, Optical and surface properties TiO<sub>2</sub> thin films deposited by DC magnetron sputtering method, *Journal of Optoelectronics and Advanced Materials* 7 (2005) 771–774.